ICSO 2016

International Conference on Space Optics

Biarritz, France

18–21 October 2016

Edited by Bruno Cugny, Nikos Karafolas and Zoran Sodnik

Radiation tests on semiconductor optical sources for space applications

P. Adamiec

L. Peñate

J. Barbero

E. Cordero

et al.

International Conference on Space Optics — ICSO 2016, edited by Bruno Cugny, Nikos Karafolas,
Zoran Sodnik, Proc. of SPIE Vol. 10562, 105620N · © 2016 ESA and CNES
CCC code: 0277-786X/17/$18 · doi: 10.1117/12.2296120

RADIATION TESTS ON SEMICONDUCTOR OPTICAL SOURCES FOR SPACE APPLICATIONS

P. Adamiec[1], L. Peñate[1], J. Barbero[1], E. Cordero[1], M. Vilera[2], I. Esquivias[2], M. Faugeron[3*], F. van Dijk[3], and M. Krakowski[3].

[1] Alter Technology TÜV Nord S.A.U., Spain. [2]Universidad Politécnica de Madrid, ETSI Telecomunicación-CEMDATIC, Spain. [3]III-V Lab Campus Polytechnique, France. [*]Now with Thales Alenia Space, France.
E-mail: pawel.adamiec@altertechnology.com.

I. INTRODUCTION

Semiconductor light sources like light emitting diodes (LEDs) or laser diodes (LDs) are the most important light sources for space applications. LEDs are used in the control panels or lightning systems in the spacecrafts and as growth lightning systems in a deep space. LDs are used as light sources for optical atomic clocks, LIDAR, optical communications, and all kind of applications where a pumping source is required as: fiber amplifiers or DPSS lasers. The most important factor for space application is the compactness of the LED or LD and their low power consumption. Since these devices need to be used in the harsh environment, different tests have to be performed. One of them is the radiation test which allows confirming if the devices can survive and work properly during the mission at chosen orbit. In case of semiconductor light sources only two tests are of interest: total ionizing dose (TID) which, in reality, cannot be screened by spacecraft shielding and the displacement damage (DD) test. TID test is performed by means of gamma radiation and it is followed by annealing period due to the fact that devices can partially or totally recovered after TID test. The DD test is usually performed by protons and the energies and fluences of interest can be found using ie. the AP8 or JPL91 models [Tylka1997, Sawyer1976, Feynman1993].

In this work we present the results of TID and DD tests on blue/violet and near infrared (NIR) LEDs. Further, the blue and NIR LDs which will be used in quantum communication tests on the 600 km sun-synchronous orbit [Liu2015] were tested for DD, since protons are the most important degradation sources at this orbit. Finally, the equivalent TID test was performed for monolithically integrated master-oscillator power-amplifier (MOPA) which was developed within the FP7 BRITESPACE project for LIDAR applications [Britespace].

II. SAMPLE DESCRIPTION

In the following subsections a description of basic parameters of the tested LEDs and LDs will be given. Almost all of them are the commercial-of-the-shelf (COTS) devices which were available at the time of the preparation of the missions. Only the monolithically integrated MOPA was a device developed especially for CO_2 sensing within BRITESPACE project [Perez2015].

A. Light Emitting Diodes

LEDs used in the experiments were commercially available devices emitting at different wavelengths. The details concerning manufacturer, basic parameters, and number of irradiated samples are given in the Table 1.

Table 1. Data of tested LEDs.

Manufacturer	Type	Wavelength	Radiation test	Basic parameters	# of samples
OSRAM	SFH 4253	850 nm	TID @ CNA	≥ 6.3 mW/sr @ 70 mA	12 (8b + 3u)
OSRAM	SFH 4253	850 nm	DD @ UCL	≥ 6.3 mW/sr @ 70 mA	12 (8b + 3u)
Exalos	EXS83KS-9810	830 nm	DD @ KVI	0.15 mW@ 120 mA	6 (3b + 3u)
Micropac	62190-301	470 nm	DD @ UCL	0.3 mW @ 20 mA	6 (3b + 3u)
SET Inc.	UVTOP255	255 nm	TID @ CNA	≥ 0.15 mW @ 20 mA	6 (3b + 3u)
SET Inc.	UVTOP255	255 nm	DD @ UCL	≥ 0.15 mW @ 20 mA	6 (3b + 3u)

CNA – Centro Nacional de Aceleradores (Spain), UCL – Catholic University Louvain (Belgium), KVI – Center for Advanced Radiation Technology (Netherlands); number of samples in the bracket indicates biased (b) and unbiased (u) samples during radiation test.

B. Laser Diodes

LDs used in the experiments were commercially available devices emitting in the blue and NIR. The details concerning manufacturer, basic parameters, and number of irradiated samples are given in the Table 2. All the samples were allocated to the displacement damage test.

Table 2. Data of the COTS LDs.

Manufacturer	Type	Wavelength	Basic parameters	# of samples
Ondax Inc.	CP-405-PLR-40-2	405 nm	25 mW @ 50 mA	2 (1b + 1u)
Qphotonics	QLD-808-150S	808 nm	80 mW @ 100 mA	2 (1b + 1u)
BWT Beijing	K808D06FA-4.00W	808 nm	2W @ 2.5 A	2 (1b + 1u)
Oclaro	BMUT5-915-02-R	915 nm	2 W @ 2.5 A	2 (1b + 1u)
JDSU	JDSU-30-7602-660	976nm	85 mW @ 150 mA	2 (1b + 1u)

Number of samples in the bracket indicates biased (b) and unbiased (u) samples during radiation test.

C. Monolithically integrated Master-Oscillator Power-Amplifier

During the EU FP7 BRITESPACE project a monolithically integrated MOPA was developed. The full description of the devices is given in [Faugeron2015] and here we just give a brief description. The device consists of three independently driven sections. First section, master-oscillator (MO), is the distributed feedback laser (DFB) which is a seed laser, the second is the modulator, and the third one is the power amplifier (PA). Due to the fact that very low reflectivity of the PA facet was demanded, the modulator section was bended, and tilted tapered PA was proposed, which allows obtaining very stable optical spectrum showing high side mode suppression ratio which is necessary for green house gases spectroscopy and LIDAR applications. Front facet was anti-reflective coated (AR<10^{-3}) whereas the rear (DFB) facet was high-reflective coated (HR = 90%). The scheme is shown in Fig.1. The laser dice is mounted on AlN submount. The epitaxial design is based on an asymmetrical cladding structure which has previously demonstrated very good performances for DFB and Fabry-Perot (FP) lasers [Faugeron2013]. This method allows decreasing drastically the internal losses due to the low overlap of the enlarged optical mode with the p-doped layers. The dilute waveguide was composed of 14 periods of InGaAsP (λ_g = 1.17 μm)/InP layers. The total waveguide was 1.53 μm thick. More details about the principle of dilute waveguide are given in [Faugeron2013a]. The epitaxial structure was grown by Metal Organic Vapor Phase Epitaxy (MOVPE) on n-type InP substrates. It includes six 8 nm thick compressively strained (0.85%) InGaAsP quantum wells and five 10 nm thick InGaAsP (λg = 1.17 μm) barriers. The measured photoluminescence peak was 1.57 μm. For the electric isolation of the different sections the intersection regions were defined by removing the metallization and the p-doped contact layer followed by the ionic implantation of the region. A measured inter-section resistance is of about 2 kΩ. A 4 μm thick gold layer was deposited onto the surface to improve heat dissipation and to allow electrical bonding with minimum damage. The MOPA is emitting at 1572 nm and the light is coming out from both, rear and front facets. The light from the rear facet is used for frequency stabilization and the light from PA facet is used in the LIDAR application.

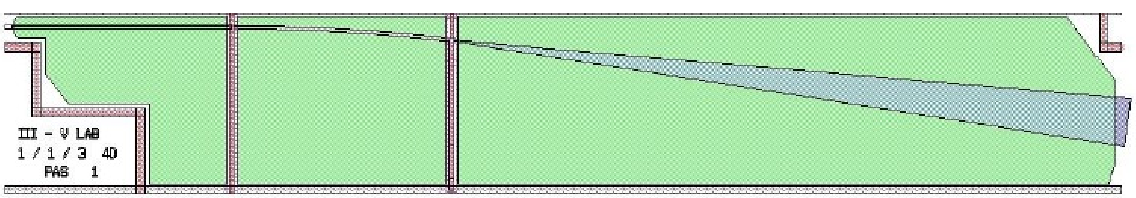

Fig. 1. Scheme of the monolithically integrated MOPA.

III. SETUP DESCRIPTION

A. Characterization of LEDs and LDs

Schematic of the measurement setup for COTS devices is shown in Fig. 2(a). The setup consists of the integration sphere where the device under test (DUT) is placed. The outputs of the sphere are connected to the power meter and optical spectrum analyzer (OSA) or spectrometer. The power meter is the Newport 2936-C, and due to the fact that sources with different wavelengths were tested, following detectors were used: Newport 818-UV for UV light, Newport 883-SL for visible and NIR, Newport 818-IG for NIR, and Newport 818P-001-02 for high power lasers. The OSA is the Antritsu MS9710C and the spectrometer Ocean Optics NIRQ512. To drive the LED and commercial LDs a Thorlabs LDC 8010 was used or precision power supply Keithley 2602B. In case of the three sections MOPA, one device was mounted and the rest were not mounted and measured in the setup with probes shown in Fig. 2(b). The DFB section was driven by LaseLock 19, the modulator and PA section were driven by means of HP Agilent 6624A when driven the mounted device and by means of Arroyo and high precision power supply Keithely 236 and HP E3631A when driven in setup with probes. The temperature of the devices was controlled by means of Peltier element and read 25°C if not explicitly stated otherwise. In case of some LEDs there was no possibility to control the temperature so they were operated in the room temperature which read 22±3°C. During the measurements the light-current-voltage (L-I-V) characteristics and spectra were measured. During the radiation the devices were placed in the custom holders which fit to the radiation beam dimensions. Due to the fact that devices were not operated or operated at low currents (below threshold in case of LDs) there was no necessity to control the temperature of the DUTs during radiation and the tests were performed at room temperature.

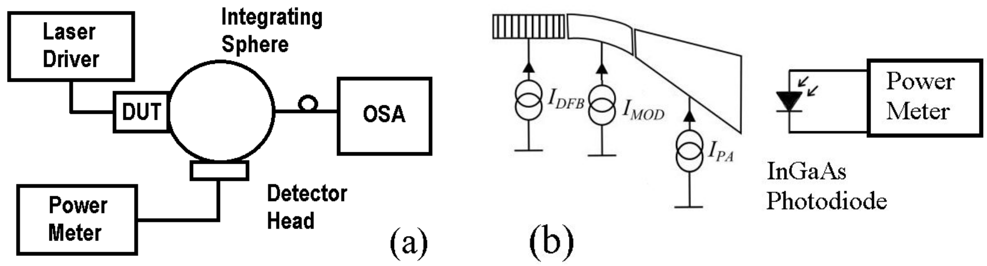

Fig. 2. The scheme of the measurement systems for COTS devices (a) and MOPA (b).

B. Radiation facilities and beam parameters

TID tests on LEDs were performed in the RADLAB in Centro Nacional de Aceleradores (CNA) in Seville, Spain. The laboratory is equipped with ^{60}Co gamma source with nominal activity of 444 TBq (12 kCi) with range of dose rate: 36 rad(Si)/h to 36 krad(Si)/h (0.36 Gy/h – 360 Gy/h). The dose rate during the test was of about 220 rad(Si)/h. The uncertainty of the dose level is below 10% and the non-uniformity of the radiation field is also less than 10%. The LEDs were irradiated up to 100 krad(Si) with several intermediate measurement steps at 10, 20, 50, and 75 krad(Si). After the irradiation they were annealed for 24 hours at the room temperature (denoted as A1) following with the second annealing at higher temperature (denoted as A2) for 168 hours.

Besides, CNA was used for irradiation of MOPAs with low energy protons of 15.168 MeV, with the flux of $1.48 \cdot 10^9$ protons/(s·cm^2), and the diameter of the beam was of about 15 mm. The MOPAs had maturity problem of the inter-electrode processing, so the duration of the standard TID is beyond the reliability of the MOPA. Therefore a solution was found connected with the fact that irradiation with low energy protons, besides displacement damage, introduces also significant TID effect. The relationship between TID and proton fluence is given by the equation [McMahan2008]:

$$\text{Dose (rad)} = \text{Fluence} \cdot \text{LET} \cdot 1.6 \cdot 10^{-8} \qquad (1)$$

where the fluence is in units of p/cm^2 and the linear energy transfer (LET) in MeV·cm^2/mg. LET is a measure of the energy deposited per unit length as an energetic particle travels through a material. The following Table 3 presents the LET, the penetration range in InP and the maximum fluence in p/cm^2 necessary for reaching an equivalent total dose of 26, 50, and 100 krad.

Table 3. Equivalent TID for irradiation of MOPAs.

Atom	Energy (MeV)	LET (MeV·cm^2/g)	Range (μm)	Equivalent TID (krad)	Max Fluence (ions/cm^2)	Flux (ions/(s·cm^2))
H+	15.168	18.29	1069	26	8.88E+10	1.48E+09
H+	15.168	18.29	1069	50	1.71E+11	1.48E+09
H+	15.168	18.29	1069	100	3.42E+11	1.48E+09

For DD test proton beams at UCL and KVI were used. At UCL a CYCLONE110 (CYClotron de LOuvain-la-NEuve) is a multiparticle, variable energy, isochronous cyclotron capable of accelerating protons up to 65 MeV. The beam diameter is of about 25 mm and the flux can be adjusted to the needs of applications. At KVI the standard proton beams used for irradiations produced by the AGOR cyclotron have primary energies in the range from 40 to 190 MeV, but at the DUT they are typically 5-10 MeV lower depending on the scatter system used. Using an energy degrader virtually all energies between 10 MeV to 184 MeV can be provided. The energy resolution of the beam when leaving the cyclotron is typically better than 0.25%. However, at the DUT position the resolution is in the order of a few MeV or more due to scatter in air, the scatter system and, when used, the energy degrader. Both circular and rectangular fields are available. The standard irradiation field has a diameter of 70 mm and homogeneity of better than ±3%. Typical fluxes are in the order of 10^8 to 10^9 p/(cm^2·s) and fluences up to 10^{13} p/cm^2 can be delivered.

IV. RADIATION RESULTS FOR LIGHT EMITTING DIODES

A. Total ionizing dose

The TID test was performed on two types of LEDs: one emitting at 850 nm and the second at 255 nm. The radiation steps were the same for both types and read: 10, 20, 50, 75, and 100 krad. The samples were measured before and after the radiation test. Besides, all of the samples were annealed at 24°C for 24 h. Then the 850 nm LEDs were annealed at 100°C for 168 h, whereas the UV ones at 55°C for 168 h, according to the maximum operation temperatures given in manufacturer datasheets. In case of 850 nm LEDs 12 samples were irradiated under the following driving conditions: 4 samples biased at 10 mA, 4 samples biased at 70 mA, and 4 unbiased. In the radiation test of 255 nm LED 3 samples were biased at 5 mA and 3 were unbiased. There was always a control sample to check the setup.

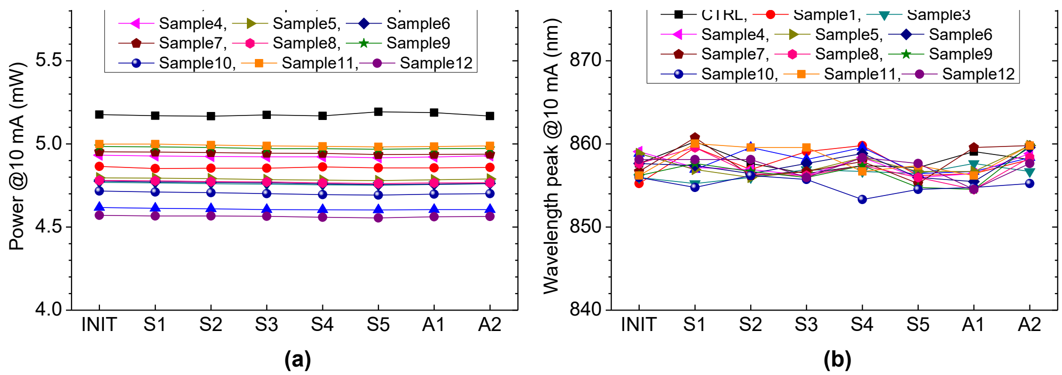

Fig. 3. Optical power (a) and wavelength (b) at peak emission for 850 nm LED at different steps: INIT – initial, S1 – 10 krad, S2 – 20 krad, S3 – 50 krad, S4 – 75 krad, S5 – 100 krad, A1 – annealing 24 hours, and A2 – annealing 168 hours.

The measurements were taken at 5 mA and 10 mA. The samples showed almost no degradation in power (below 1%) and the emission wavelength was changing independently on radiation level about 1.5 nm as can be seen from Fig. 3. Similar measurements were performed for UV LEDs. The results for both types of LEDs are shown in Table 4. The degradation in the output power is below 1% and 1.43% for 850 nm and 255 nm LEDs, respectively. There was no significant difference between the obtained results for biased and unbiased samples.

Table 4. Results of TID test for 850 nm and 255 nm LEDs.

Parameter for 850 nm LED		Bias conditions during radiation		
		10 mA	70 mA	UNBIAS
Reduction of optical power (%)	At 5mA	0.95	0.87	0.80
	At 10mA	0.39	0.38	0.39
Change of spectrum	Maximum peak (nm)	1.02	1.74	0.54
	Centroid (nm)	0.72	0.72	1.07
Parameter for 255 nm LED		Bias conditions during radiation		
		5 mA		UNBIAS
Reduction of optical power (%)	At 5mA	1.43		1.42
	At 10mA	1.25		1.25
Change of spectrum	Maximum peak (nm)	0.35		0.32
	Centroid (nm)	1.72		1.27

B. Displacement damage

Displacement damage test was performed on four types of LEDs emitting at 850 nm, 830 nm, 470 nm, and 255 nm by means of protons with energy of 60 MeV. The final fluence was $8{\cdot}10^{11}$ p/cm^2 with the intermediate steps at $1{\cdot}10^{11}$, $4{\cdot}10^{11}$, $6{\cdot}10^{11}$ p/cm^2 for samples at 850 nm, 470 nm, and 255 nm. 830 nm LED was tested at $2.5{\cdot}10^{10}$, $5{\cdot}10^{10}$, $7.5{\cdot}10^{10}$ $10{\cdot}10^{10}$, $20{\cdot}10^{10}$ p/cm^2. The examples of output power level and wavelength peak during the radiation are shown in Fig. 4. It can be seen that the wavelength is changing within ±1 nm independently of the fluence whereas the output power degrades with increasing fluence. Finally, about 25% drop of the output power after the last step was measured for the sample which was unbiased during the radiation test. The data for other LEDs after the final fluence are gathered in Table 5. In all cases the wavelength change is within the measurement error, but the output power is degrading with increasing fluence. All unbiased LEDs have shown higher percentage degradation of the output power than the biased devices. This can be attributed to the fact that besides the DD effect also the TID occurs which is less pronounced in the biased devices due to the annealing effect. The other observation is that the degradation is more visible at lower current excluding the 830 nm LED.

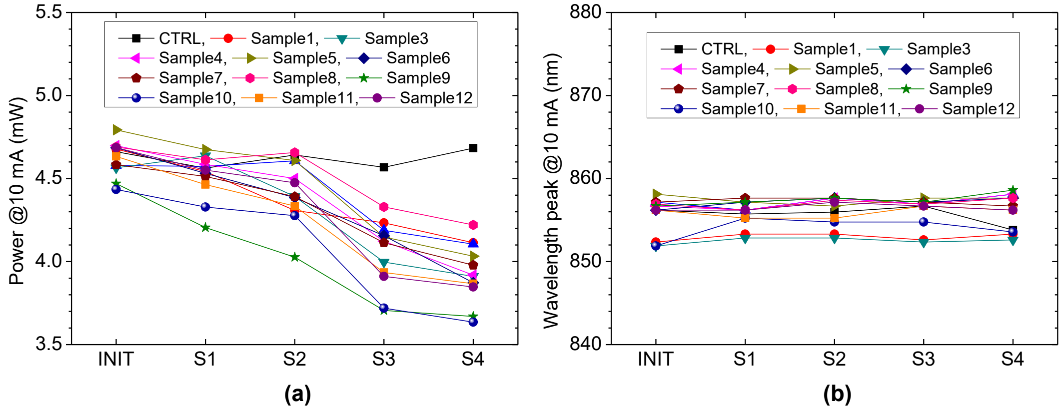

Fig. 4. Optical power (a) and wavelength at peak emission (b) during the DD test for 850 nm LED.

Table 5. Results of the DD test for COTS LEDs.

Sample	Driving current (mA)	Output power drop during radiation (%) biased	Output power drop during radiation (%) unbiased
850 nm (SFH4253)	5	19.6	25.5
	10	13.3	17.6
830 nm (EXS83KS-9810)	30	5.1	5.2
	40	7.1	9.4
470 nm (62190-301)	5	4.6	5.7
	10	4.5	5.6
255 nm (UVTOP255)	5	4.5	9.3
	10	3.8	8.4

V. RADIATION RESULTS FOR LASER DIODES

In the first part of this section the results of DD tests of COTS lasers will be shown then in the second part following with the results for MOPA. The COTS lasers will be used on the polar orbit for quantum communication purposes. The required level for the 2 year mission is below $1{\cdot}10^{10}$ p/cm^2 for protons of the energy higher than 10 MeV [Liu2015]. Therefore in the experiment 50 MeV protons were used with fluence up to $1{\cdot}10^{12}$ p/cm^2 to have enough safety margin. The measurements were taken for pristine devices and then during the intermediate steps: Step 1 (S1) – $1{\cdot}10^{9}$ p/cm^2, Step 2 (S2) – $1{\cdot}10^{10}$ p/cm^2, Step 3 (S3) – $1{\cdot}10^{11}$ p/cm^2, and Step 4 (S4) – $1{\cdot}10^{12}$ p/cm^2. Fig. 5 shows the L-I characteristics for 5 different COTS LDs. The left column corresponds to the unbiased samples whereas the right column to the biased ones. The biased samples were driven at value of 120 % of the threshold current which reads: 30 mA for CP-405-PLR-40-2, 41 mA for QLD-808-150S, 960 mA for K808D06FA-4.00W, 520 mA for BMUT-815-02-R, and 30 mA for JDSU-30-7602-660. At a glance, the unbiased devices have more complex response than the biased devices which is again the influence of the annealing when LDs were operated during radiation. As can be seen from Fig. 6 (left) during first three steps the threshold current is unchanged and increases slightly at the highest fluence. The wavelength is constant during all radiation steps independently of the driving conditions during radiation (see the right part of Fig. 6).

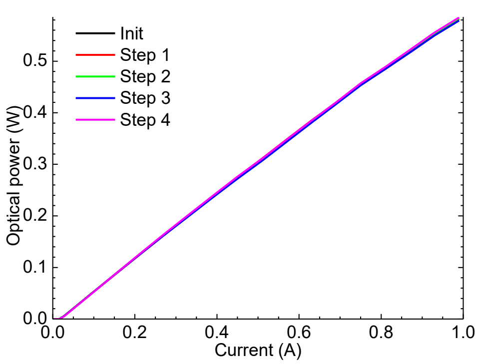

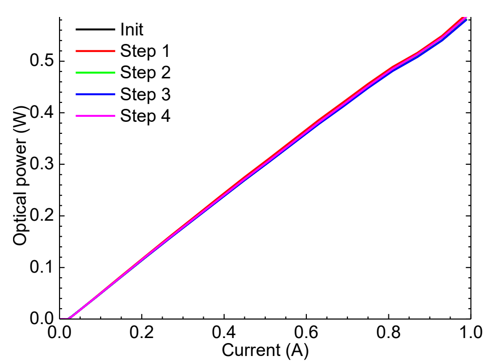

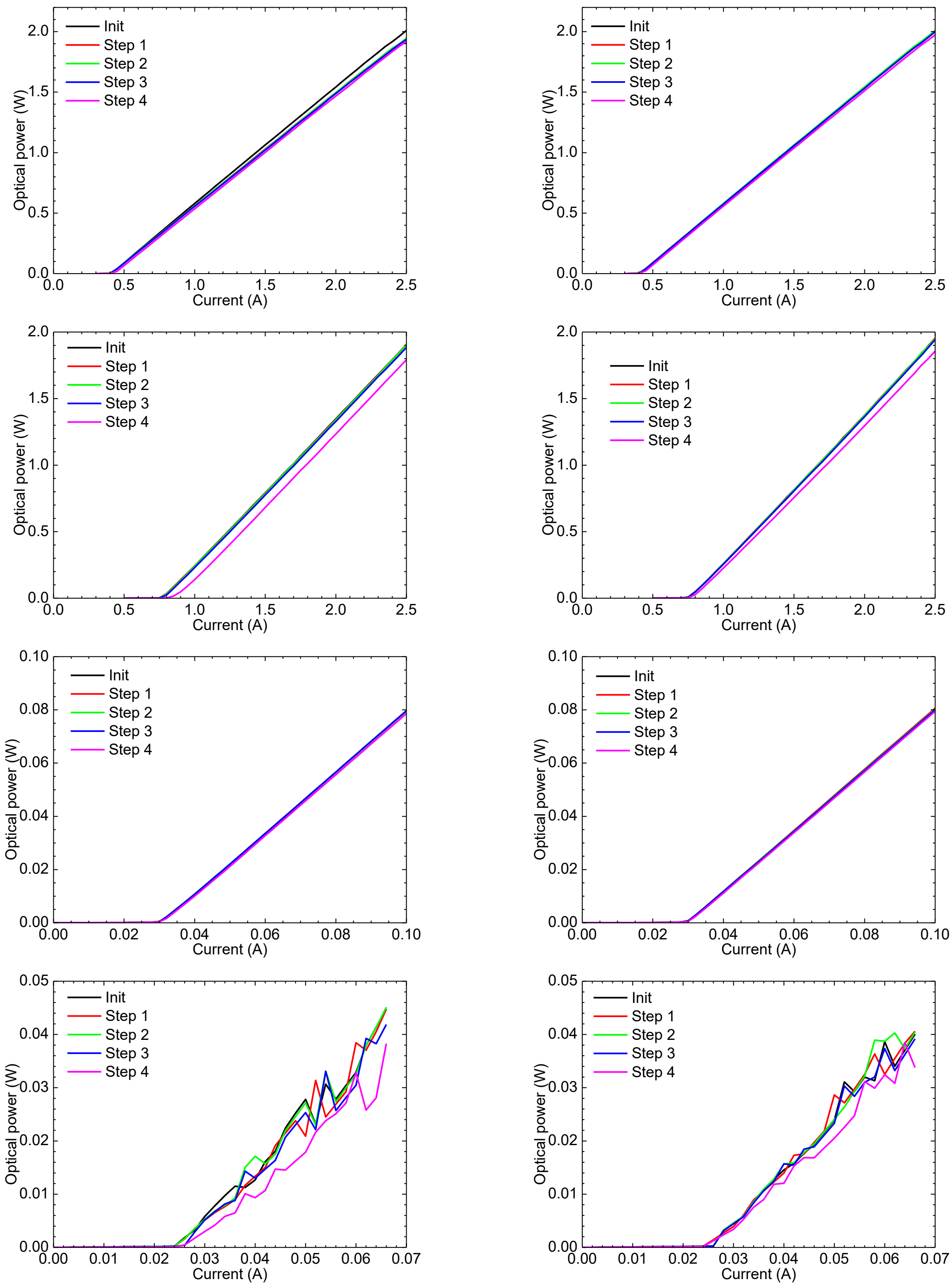

Fig. 5. Light-current characteristics for COTS LDs. Unbiased (left) and biased (right). From the top to bottom: JDSU-30-7602-660 at 976 nm, BMUT-815-02-R at 915nm, K808D06FA-4.00W at 808 nm, QLD-808-150S at 808 nm, and CP-405-PLR-40-2 at 405 nm.

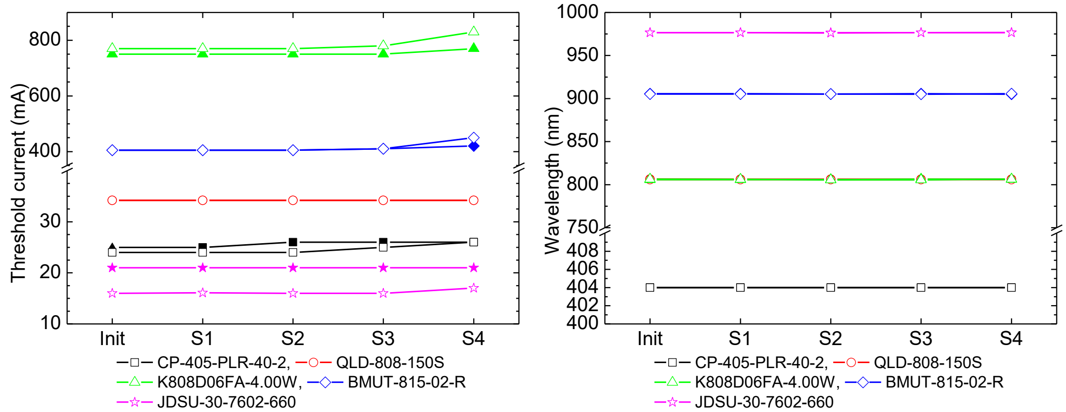

Fig. 6. Threshold currents (left) and wavelength (right) for COTS LDs in the function of radiation steps. Opens symbols corresponds to unbiased devices and full symbols to biased ones.

Since the MOPAs inter-electrode processing problems resulting in the MOPA short lifetime it was necessary to find a way to overcome the long duration time of the TID to check the radiation hardness of the material. As aforementioned in the section II.B the equivalent TID method was used and the MOPAs were irradiated with the 15 MeV protons (see Table 3 for fluence levels). All MOPAs were unbiased during radiation test. The MOPA which targeted the highest TID of 100 krad has degraded, but it was not possible to distinguish if the degradation was a result of irradiation or degradation due to the manufacturing problems. The two other devices were tested to equivalent TID of 26 krad (M08-0082) and 50 krad (M08-134). Both MOPAs were measured by means of probes and the light was collected on the InGaAs photodiode from the DFB facet. The L-I curves taken at 15°C are shown in the Fig. 7. During these measurements the DFB current was limited to 200 mA, the modulator section was driven only at 5 mA, and the PA section at 100 mA, to avoid degradation. It can be seen that the threshold currents are unchanged and the slopes after radiation are even higher than before, but this could be due to the different photodiode and MOPA orientation during the measurements after the radiation test. The most important information is given by the voltage-current (V-I) characteristics in the region when the voltage is in the range when the p-n junction is still closed. Any changes in the V-I in this region indicate change in the material. As it can be seen in the Fig. 7 the V-I characteristic is unchanged from 0 V to 0.7 V, which confirms that there is no degradation in the material.

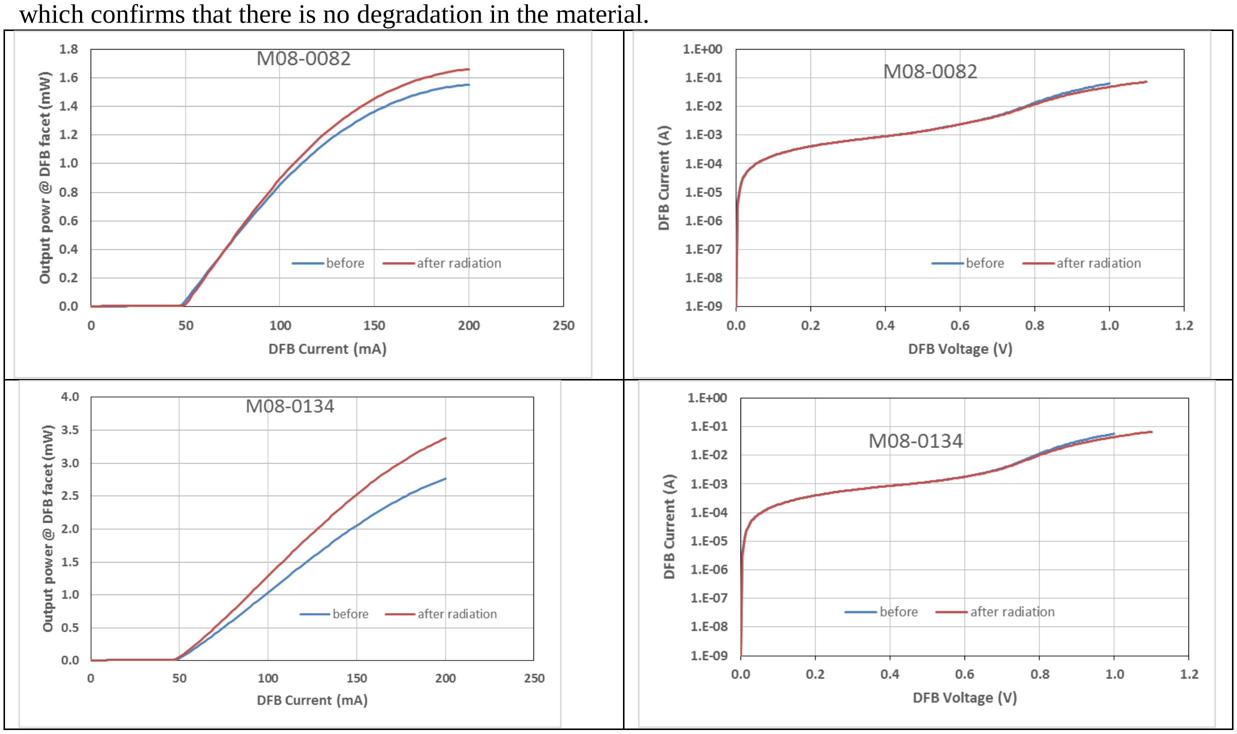

Fig. 7. L-I and V-I characteristics for DFB section of the MOPA.

VI. SUMMARY AND CONCLUSIONS

Different semiconductor optical sources for space applications have been tested by means of TID and DD. Commercially available LEDs and LDs were tested by means of 50 – 60 MeV protons up to fluence of $1\cdot10^{12}$ p/cm^2 with several steps for intermediate measurements to study the displacement damage effects. Additionally, LEDs were submitted to the TID test up to cumulative doses of 100 krad. LEDs showed no deterioration of the characteristics after the TID test whereas a decrease of the output power was found after the DD test. This decrease depends on the operating wavelength of the devices. LEDs operating in the NIR region showed 25% drop of the output power and in the blue/violet region up to 10%. There was no change in the emission wavelength. All unbiased LEDs during radiation have shown higher percentage degradation of the output power than the biased devices. This can be attributed to the fact that besides the DD effect also the TID occurs which is less pronounced in the biased devices due to the annealing effect. Tested commercial LDs did not experienced any degradation of characteristics up to fluences of $1\cdot10^{11}$ p/cm^2, but showed slight increase in the threshold currents and decrease of the output power when the fluences reached $1\cdot10^{12}$ p/cm.^{2} Devices emitting in the NIR wavelengths showed up to 10% drop of the output power and those emitting in the blue range showed up to 20% decrease of the output power. Apart of the commercial lasers a three section MOPAs designed and manufactured by III-V labs within the frame of the FP7 project BRITESPACE were tested by means of low energy protons. The energy was 15 MeV and fluences were adjusted to reach the equivalent total dose of 50 krad. The output power and threshold currents of the master-oscillator (DFB) remained constant which confirms that the material and technology of this monolithically integrated high power devices emitting at 1572 nm are adequate for space applications.

REFERENCES

[Tylka1997] A.J. Tylka, James H. Adams, Jr., Paul R. Boberg, Buddy Brownstein, William F. Dietrich, Erwin O. Flueckiger, Edward L. Petersen, Margaret A. Shea, Don F. Smart, and Edward C. Smith, "CREME96: A Revision of the Cosmic Ray Effects on Micro-Electronics Code", IEEE Transactions on Nuclear Science, 44, 2150-2160 (1997); and references therein.

[Sawyer1976] Sawyer, D. and J. Vette, "AP-8 trapped proton environment for solar maximum and solar minimum," National Space Science Data Center, Report 76-06, Greenbelt, Maryland, 1976.

[Feynman1993] Feynman, J., G. Spitale, J. Wang, and S. Gabriel, "Interplanetary Proton Fluence Model: JPL 1991, " J. Geophys. Res., 98, 13,281-13,294, 1993.

[Liu2015] H. Liu, H. Jiang, Y. Shen, S. Liao, J. Yin, Y. Cao, Y. Liu, and R. Zhu, "Displacement Damage Test on COST Laser Diodes Embedded in Satellite", Proc. of RADECS 2015, paper DW-21.

[Britespace] http://www.britespace.eu.

[Perez2015] A. Pérez-Serrano, M. Vilera, I. Esquivias, M. Faugeron, M. Krakowski, F. van Dijk, G. Kochem, M. Traub, P. Adamiec, J. Barbero, X. Ai, J. Rarity, M. Quatrevalet, and G. Ehret. "Atmospheric CO2 Remote Sensing System based on High Brightness Semiconductor Lasers and Single Photon Counting Detection". Proc. SPIE 9645, Lidar Technologies, Techniques, and Measurements for Atmospheric Remote Sensing XI, 964503 (2015); doi:10.1117/12.2194345.

[Faugeron2015] M. Faugeron, M. Vilera, M. Krakowski, Y. Robert, E. Vinet, P. Primiani, J. P. Le Goëc, O. Parillaud, A. Pérez-Serrano, J. M. G. Tijero, G. Kochem, M. Traub, I. Esquivias and F. Van Dijk, "High Power Three-Section Integrated Master Oscillator Power Amplifier at 1.5 µm", IEEE Photonics Technology Letters, Vol. 27, Issue 13, pp. 1449-1452 (2015)

[Faugeron2013] M. Faugeron et al., "High peak power, narrow RF linewidth asymmetrical cladding quantum-dash mode-locked lasers," IEEE J. Sel. Topics Quantum Electron., vol. 19, no. 4, (2013), Art. ID 1101008.

[Faugeron2013a] M. Faugeron et al., "High-power tunable dilute mode DFB laser with low RIN and narrow linewidth," IEEE Photon. Technol. Lett., vol. 25, no. 1, pp. 7–10, Jan. 1, 2013.

[McMahan2008] M.A. McMahan, E. Blackmore, E. W. Cascio, C. Castaneda, B. von Przewoski, and H. Eisen, "Standard Practice for Dosimetry of Proton Beams for use in Radiation Effects Testing of Electronics", Proc. of 2008 IEEE Radiation Effects Data Workshop, pp. 135 - 141 (2008)